SUPPORTING INFORMATION

High Magnetization Reversal Barriers in Luminescent Dysprosium Octahedral and Pentagonal Bipyramidal Single-Molecule Magnets based on fluorinated alkoxides ligands

Jérôme Long*,[a] Aleksei O. Tolpygin,[b,c] Dmitry M. Lyubov,[b,c] Natalia Yu. Rad'kova,[b] Anton V. Cherkasov,[b] Yulia V. Nelyubina,[c] Yannick Guari,[a] Joulia Larionova[a] and Alexander A. Trifonov*[b,c]

[a] *ICGM, Univ. Montpellier, CNRS, ENSCM, Montpellier, France. E-mail: jerome.long@umontpellier.fr*

[b] *Institute of Organometallic Chemistry of Russian Academy of Sciences, 49 Tropinina str., GSP-445, 630950, Nizhny Novgorod, Russia. E-mail: trif@iomc.ras.ru*

[c] *A.N.Nesmeyanov Institute of Organoelement Compounds of Russian Academy of Sciences, 28 Vavilova str., 119334 , Moscow, Russia.*

TABLE OF CONTENTS

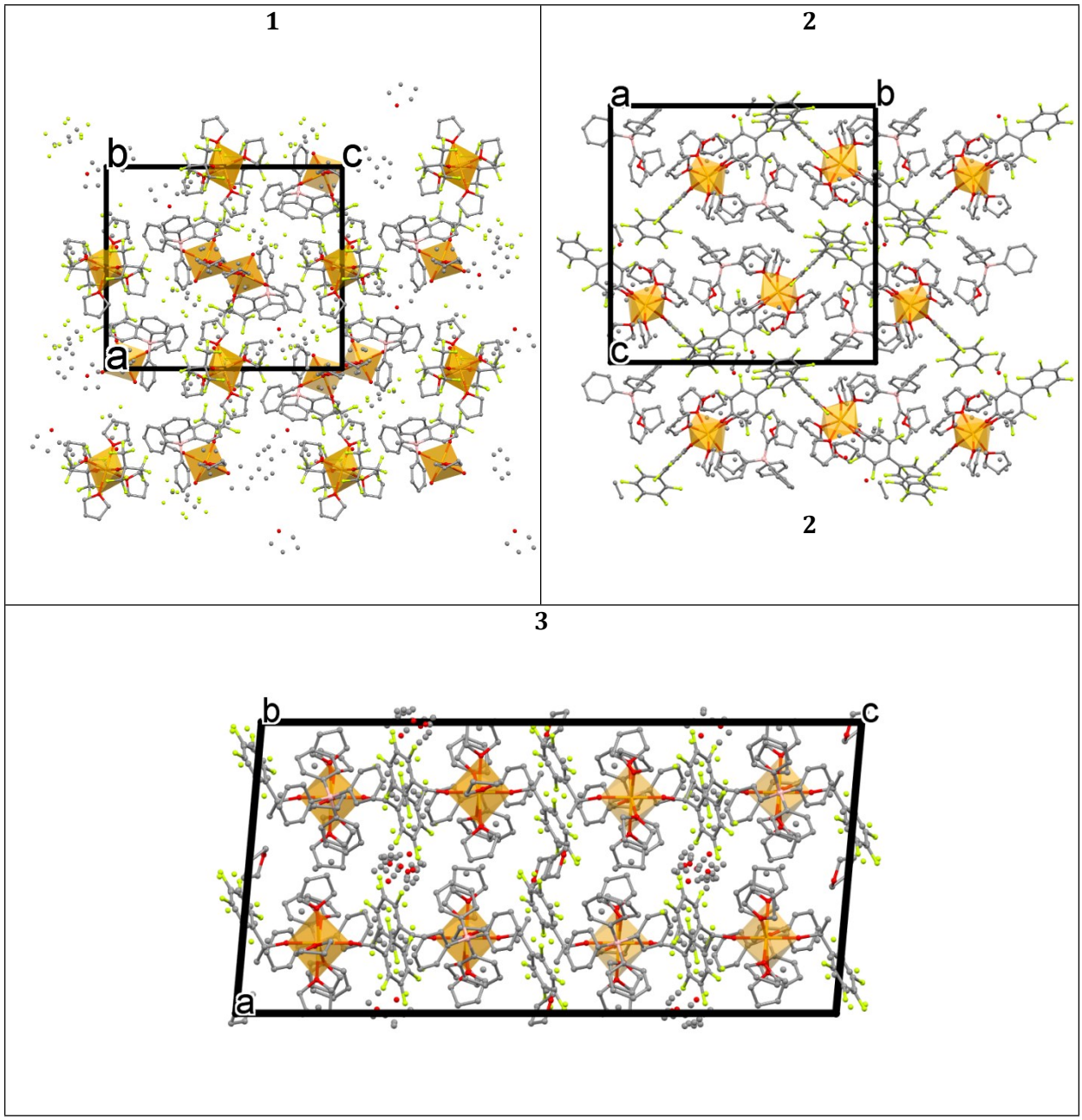

Figure S1: Perspective view of the crystal packing for **1, 2** and **3** along the *b* and *a* crystallographic axes. Hydrogen atoms have been omitted for clarity**.**

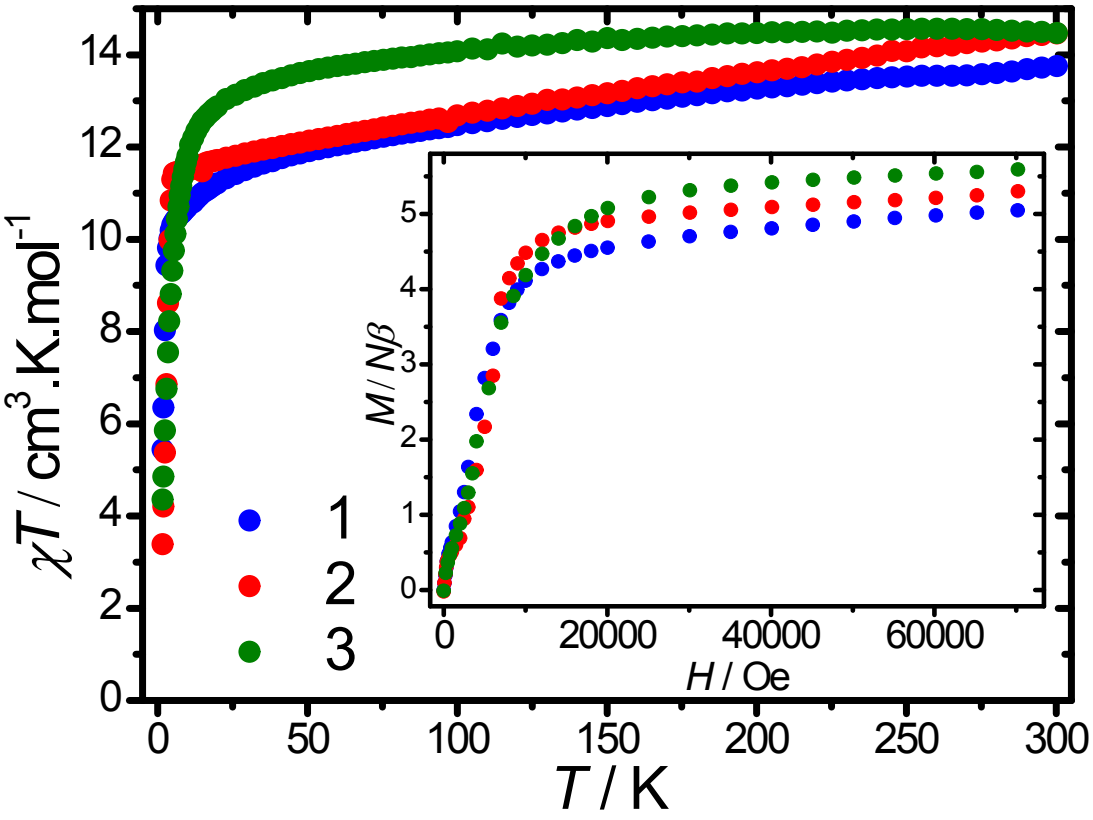

Figure S2: Temperature dependence of χT under an applied magnetic field of 1000 Oe (**1** and **2**) or 10000 Oe field (**3**). The measurement under a 1000 Oe field for **3** gives a higher χT value to a temperature independent paramagnetic contribution, which should be diminished under larger field.[1] Inset: field dependence of the magnetization at 1.8 K for **1-3**.

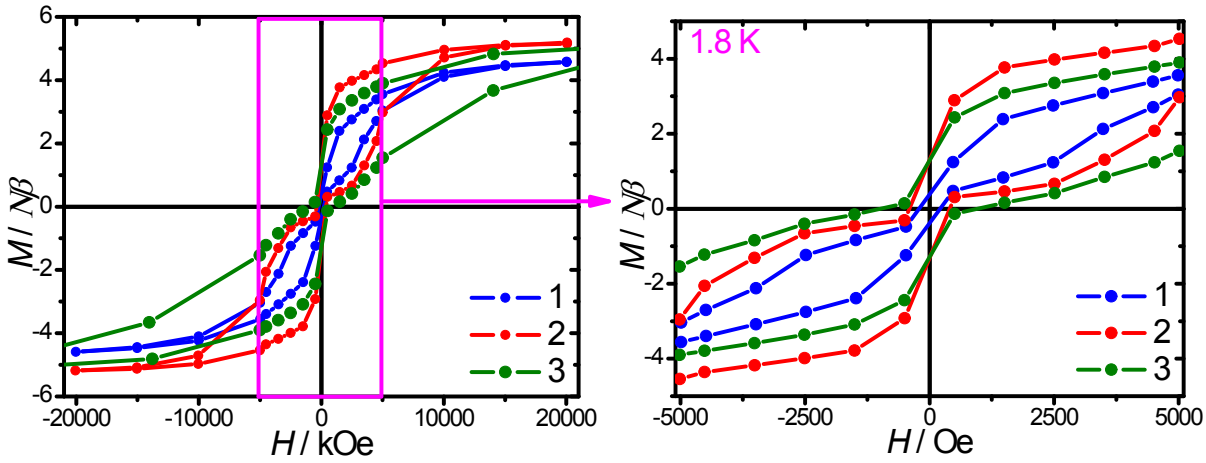

Figure S3: Hysteresis loops obtained at 1.8 K for **1**–**3** at an average sweep rate of 17 Oe·s^{-1}.

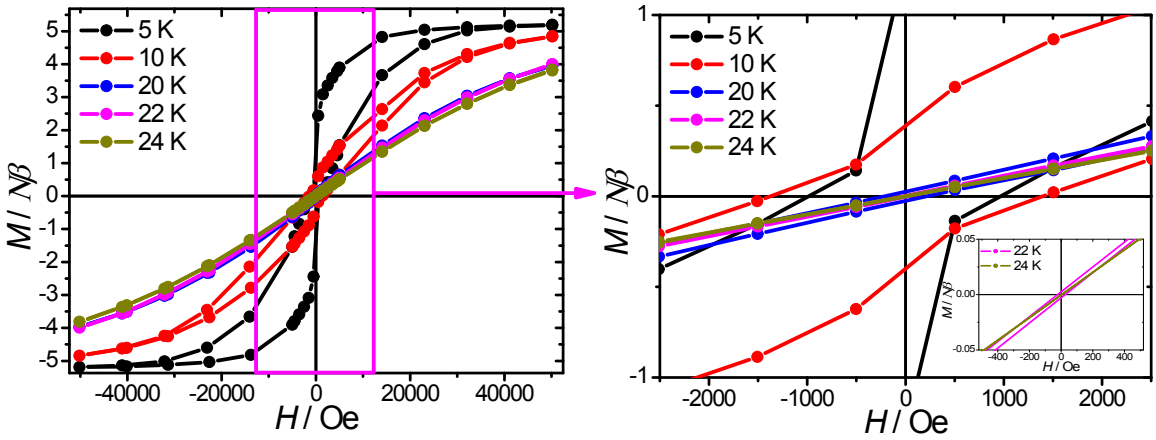

Figure S4: Hysteresis loops obtained at various temperature for **3** at an average sweep rate of 20 Oe·s^{-1}.

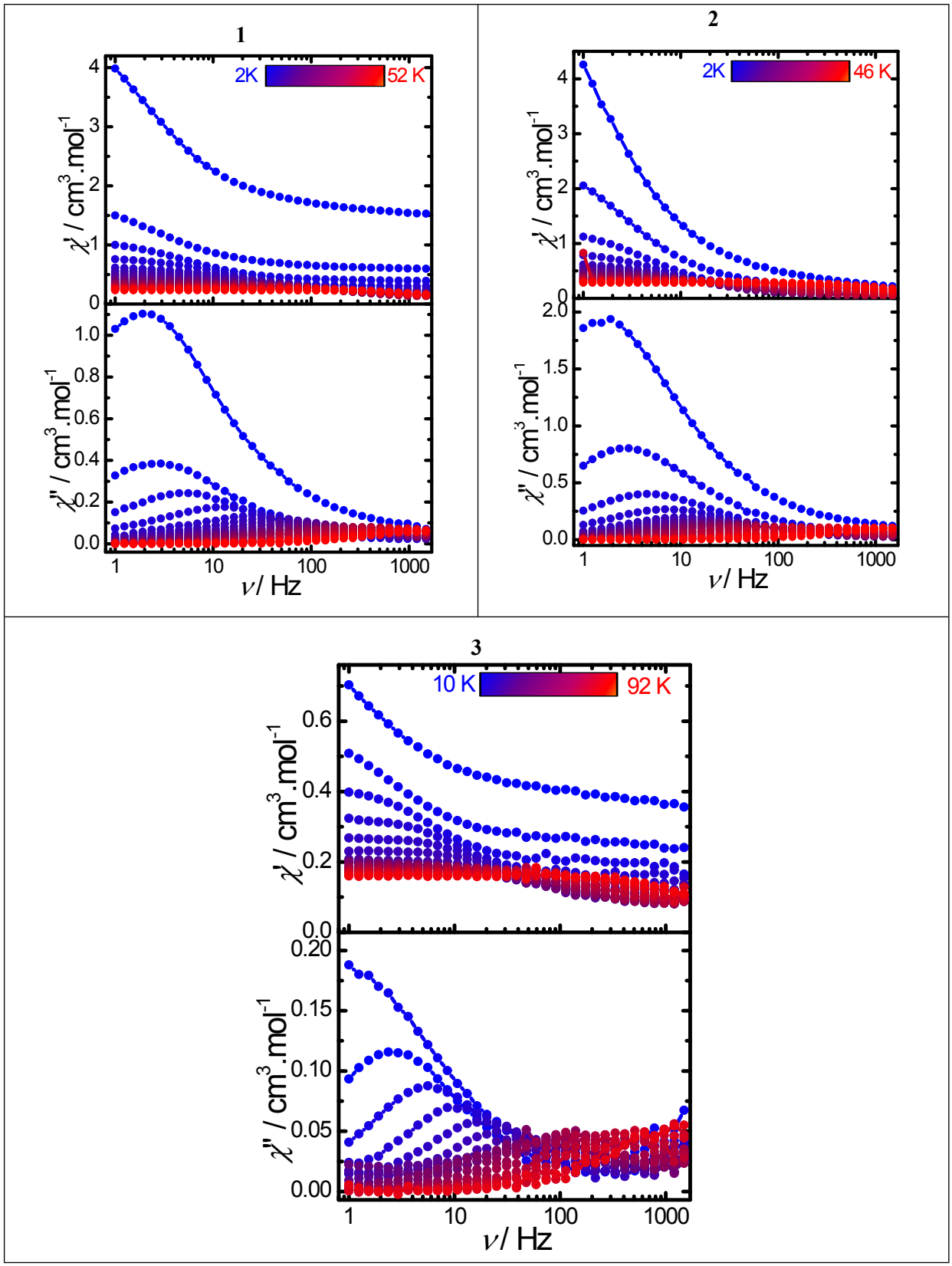

Figure S5: Frequency dependence of χ' and χ'' for **1**–**3** for different temperatures performed in zero magnetic static field.

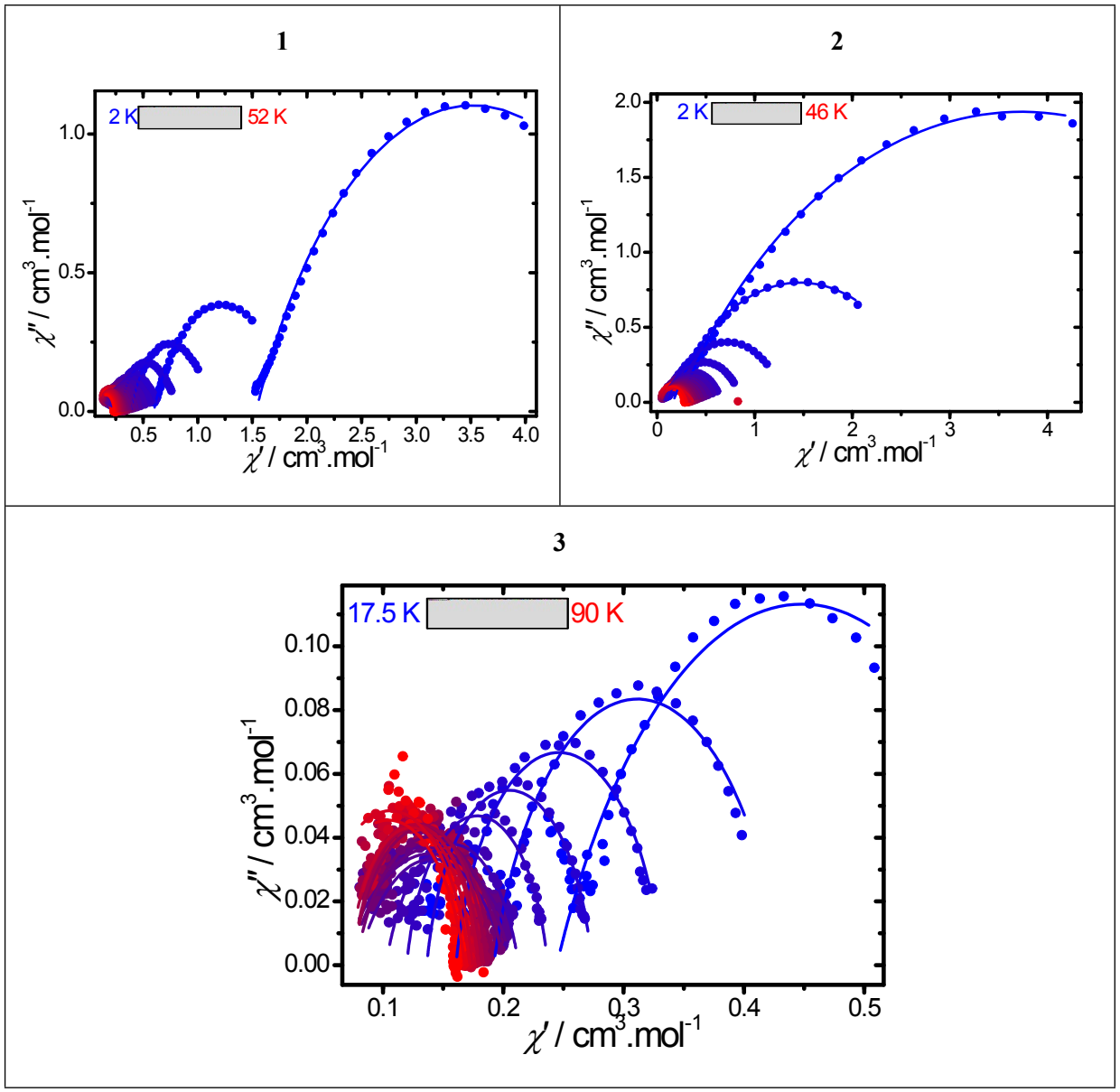

Figure S6: Cole-Cole (Argand) plots obtained using the ac susceptibility data for **1-3** in zero magnetic field. The solid lines correspond to the best fit obtained with a generalized Debye model.

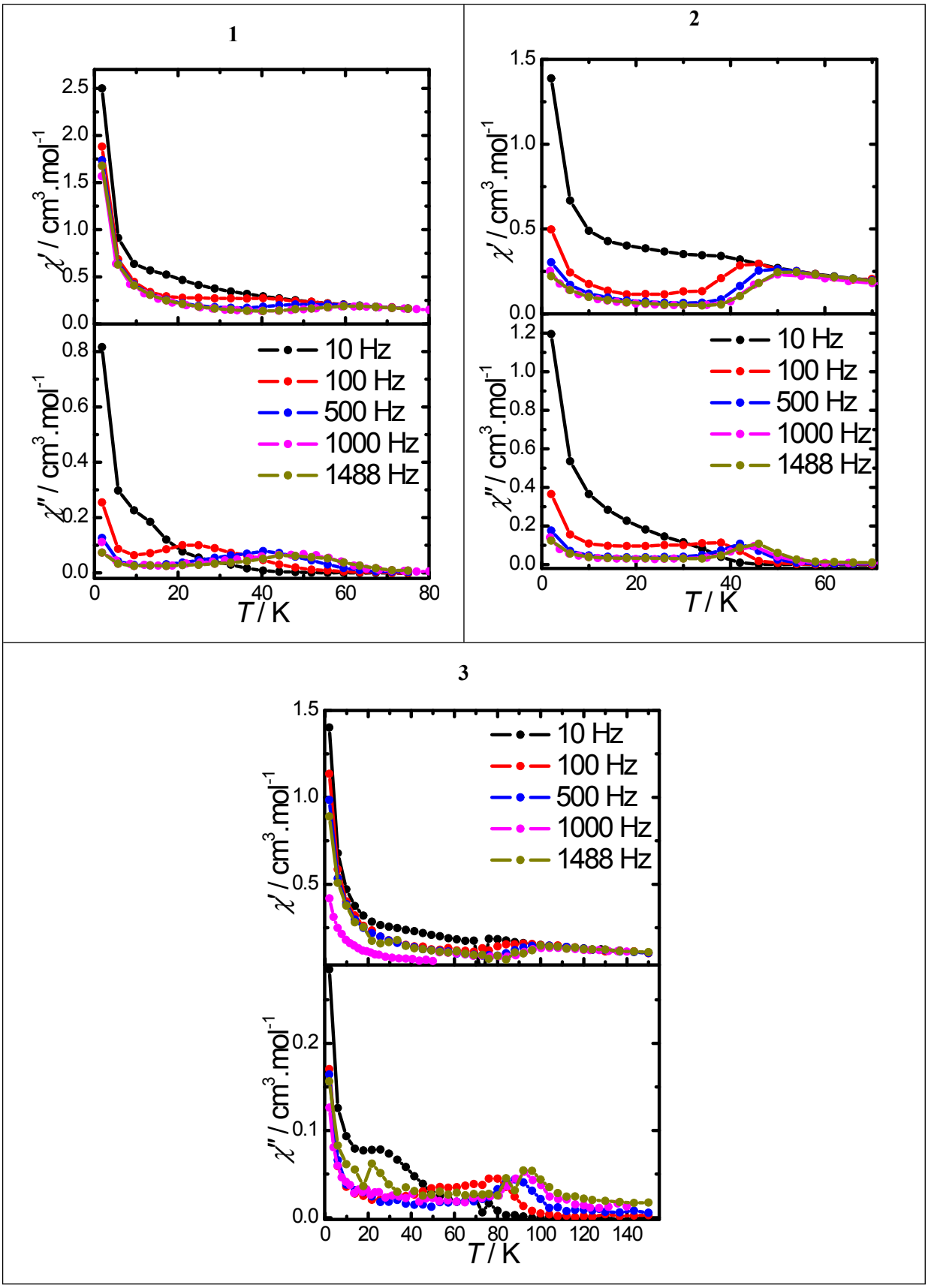

Figure S7: Temperature dependence of χ' and χ'' for **1-3** with different frequencies in zero applied magnetic field.

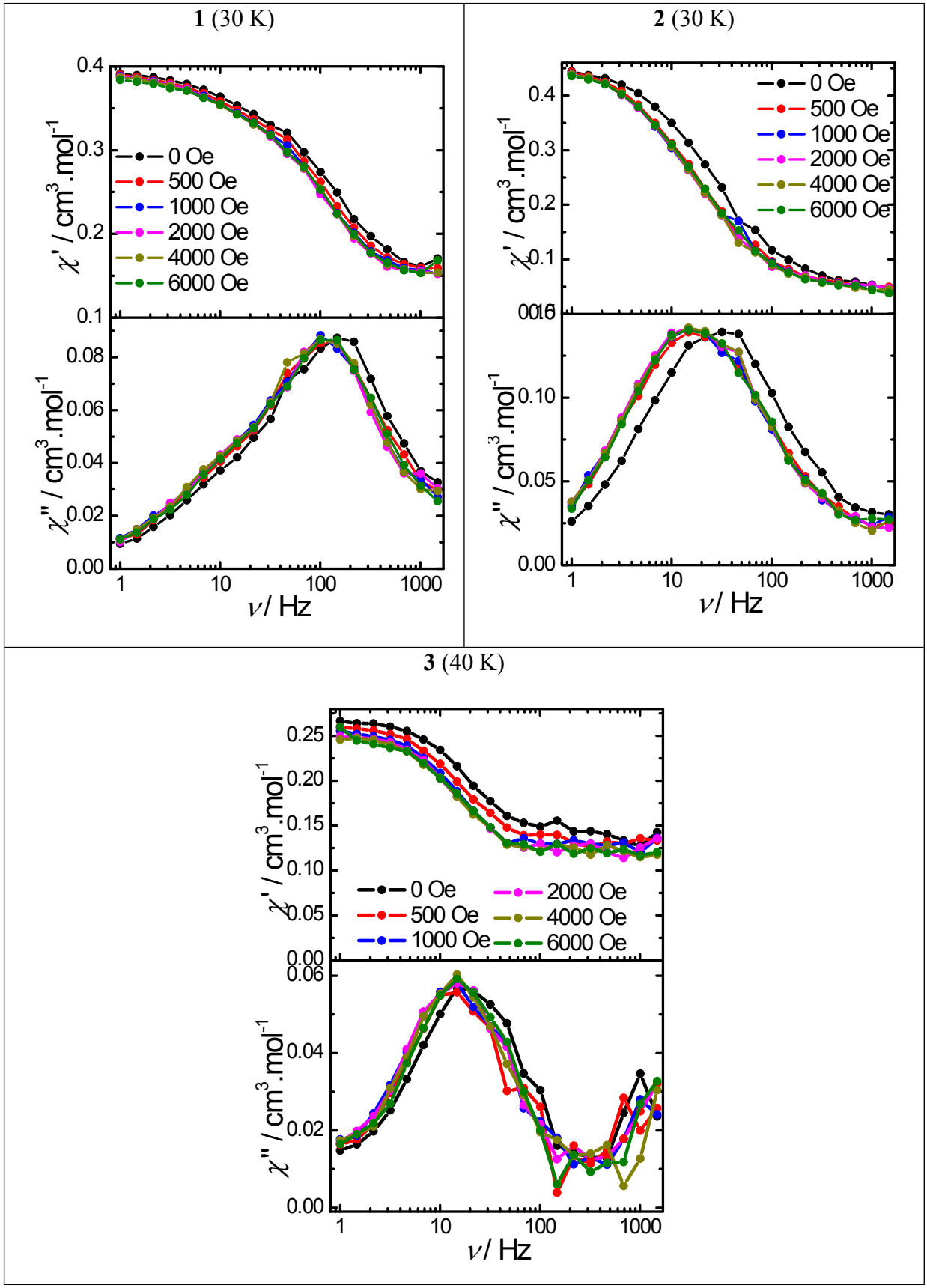

Figure S8: Frequency dependence of χ' and χ'' for **1-3** for various dc fields.

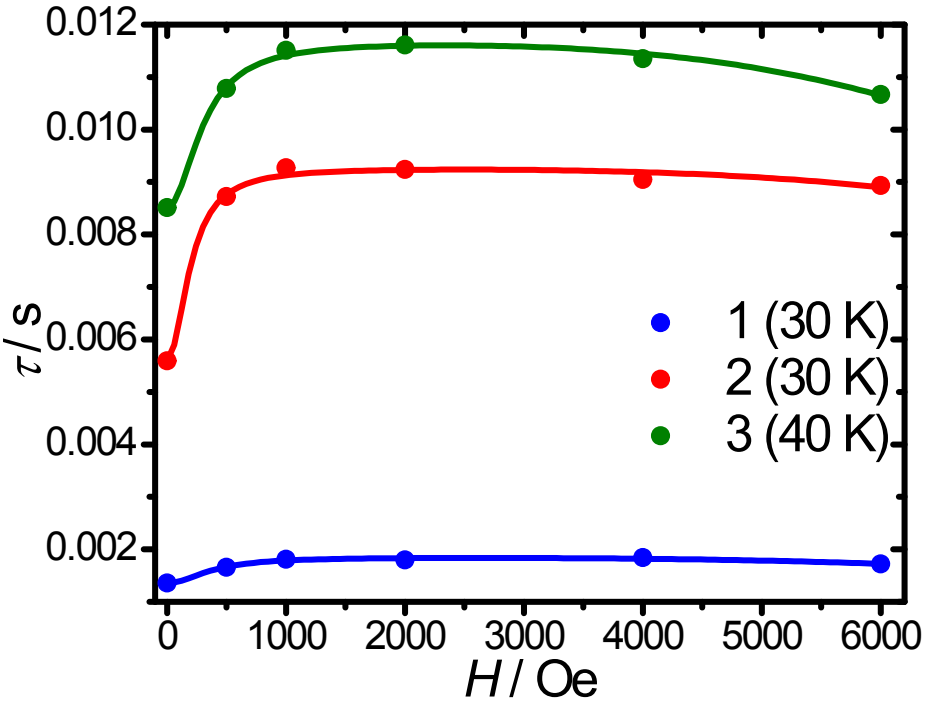

Figure S9: Field dependence of the relaxation time for **1** and **2** at 30 K. The solid lines represent the fit with Eq. 2.

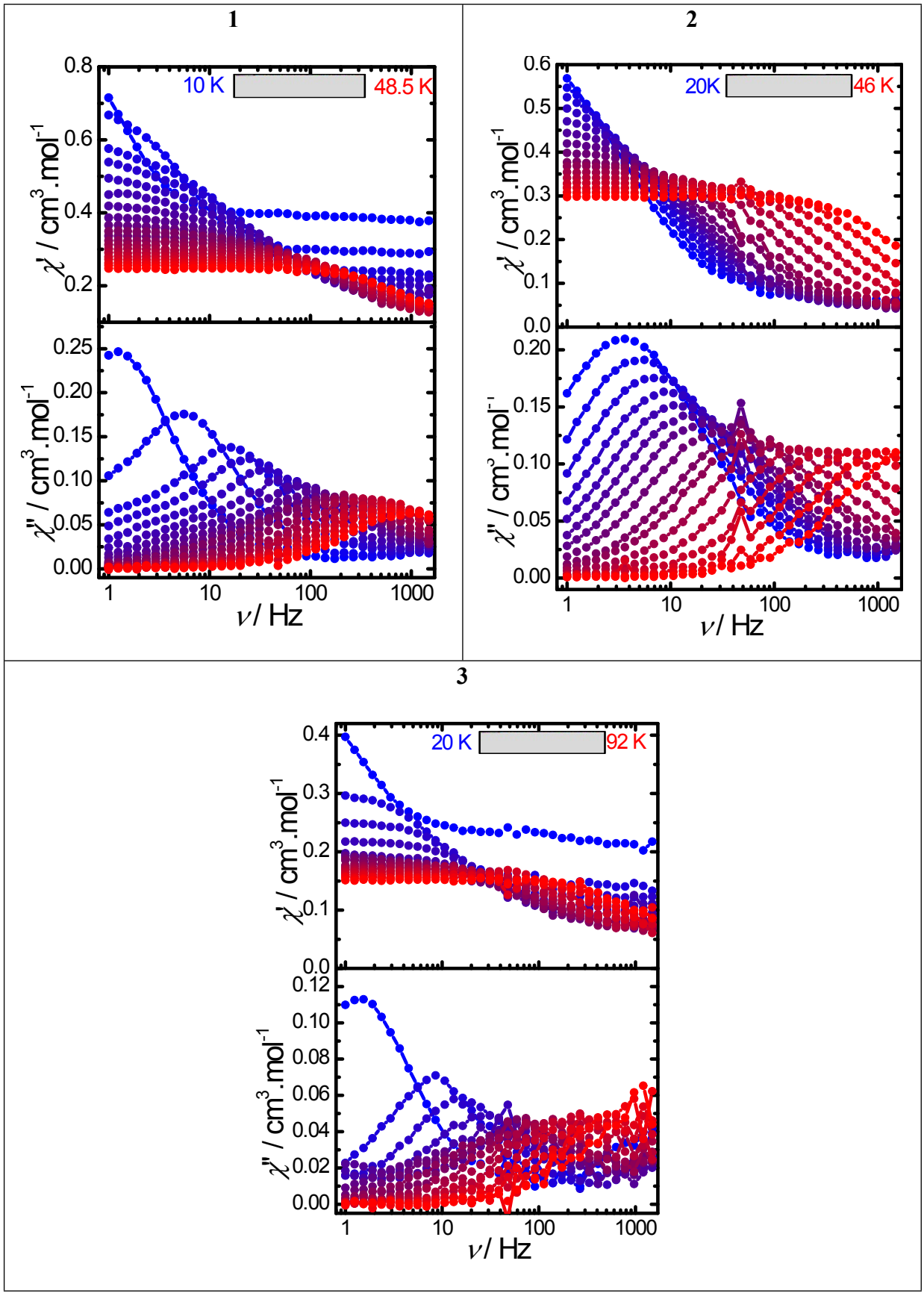

Figure S10: Frequency dependence of χ' and χ'' for **1-3** under a 1000 Oe dc field.

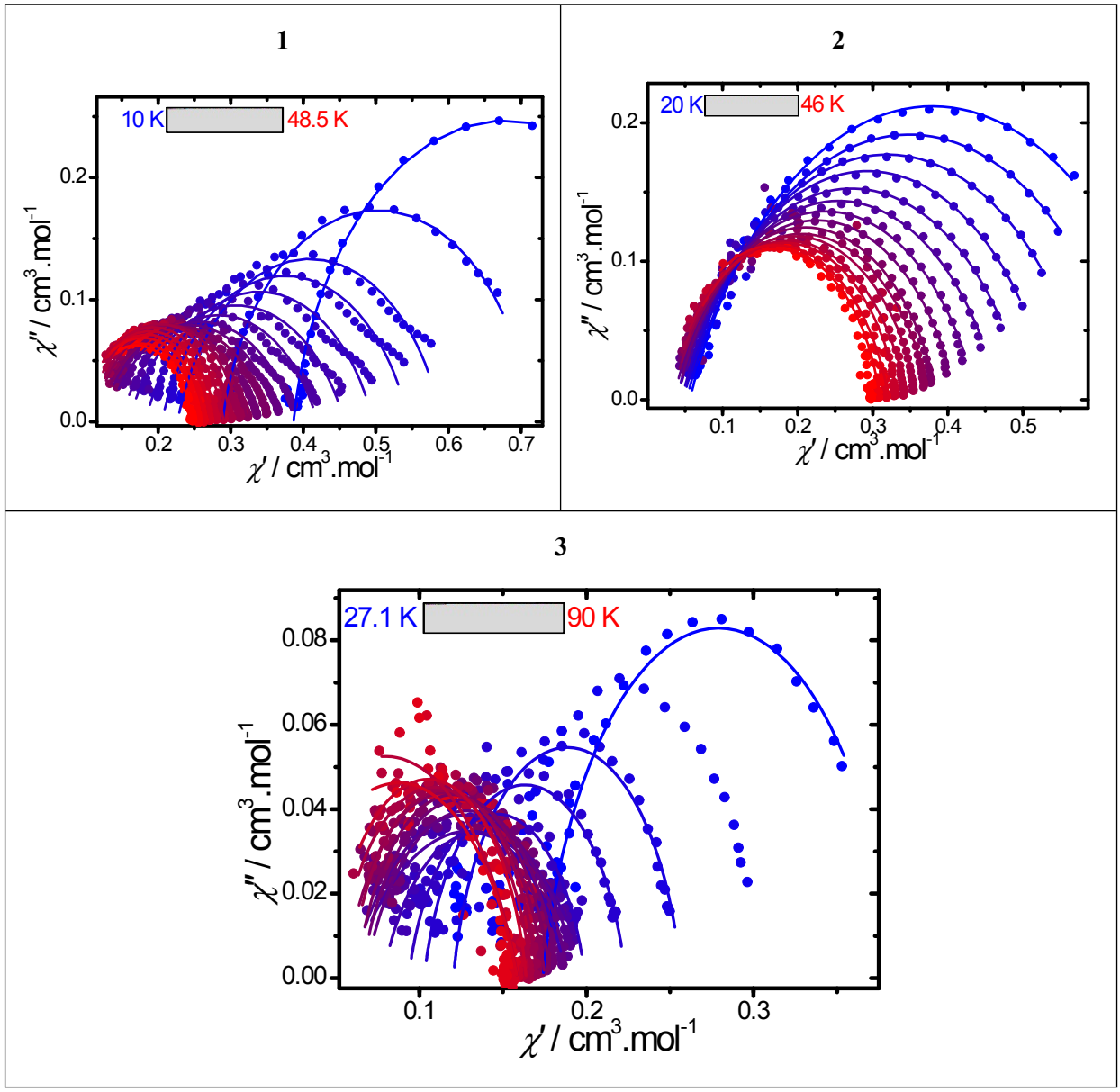

Figure S11: Cole-Cole (Argand) plot obtained using the ac susceptibility data for **1**-**3** (1000 Oe). The solid lines correspond to the best fit obtained with a generalized Debye model.

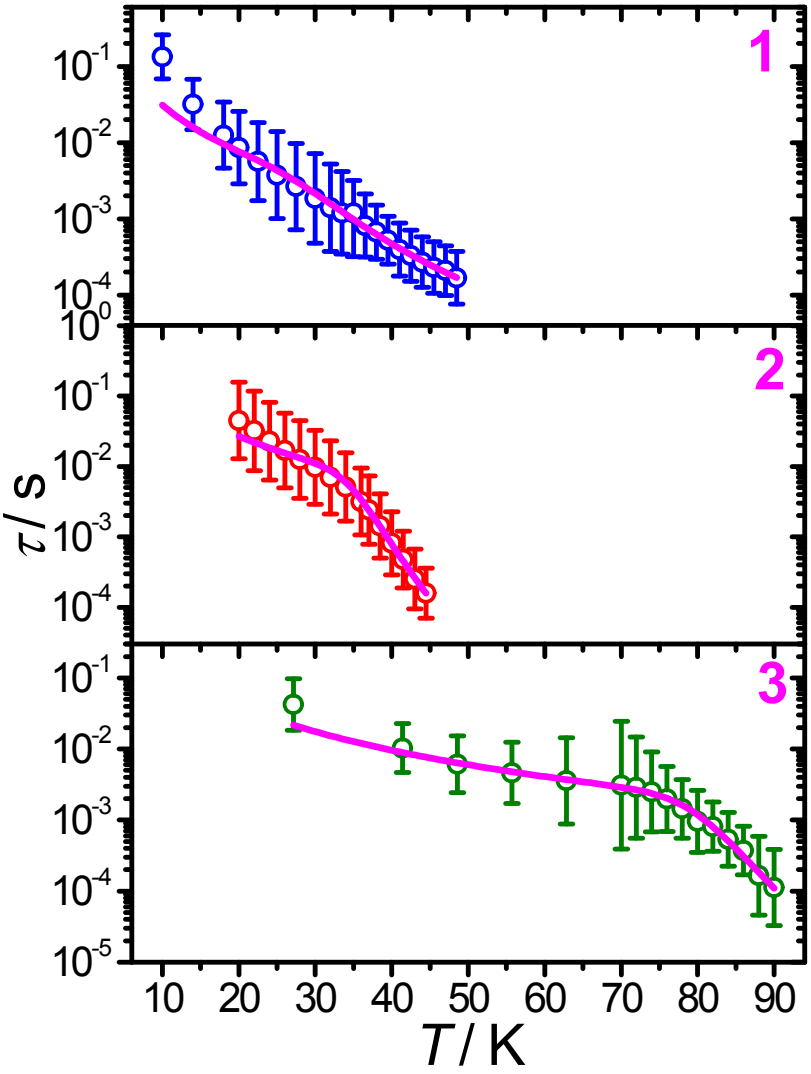

Figure S12: Temperature dependence of the relaxation time for **1-3** using the ac data at 1000 Oe. The solid line represents the fit The uncertainties were determined from the CC-FIT2 software[2] while the magenta solid lines correspond to the fit with Eq. 3 (1000 Oe).

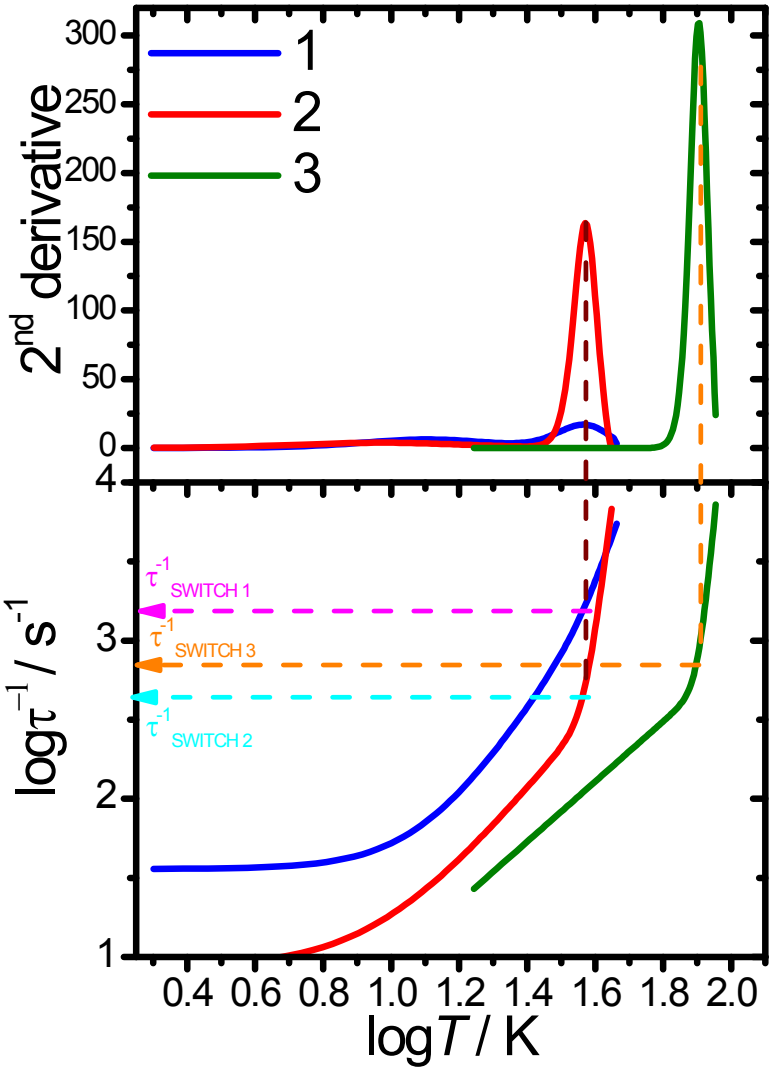

Figure S13: Temperature dependence of the relaxation time plotted as $\log\tau^{1}$ *vs.* log*T*. The second derivative allows the determination of the τ_{switch}.

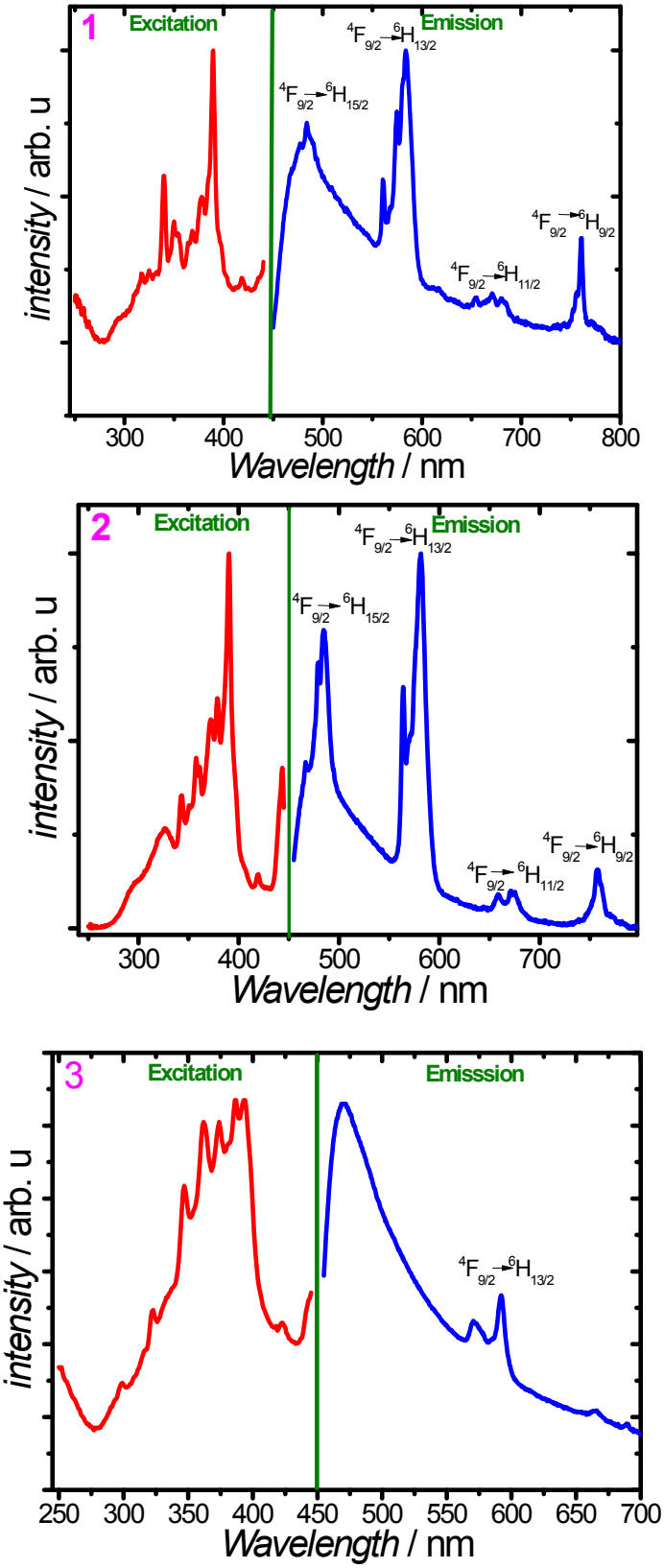

Figure S14: Room temperature normalized excitation spectra monitored at $\lambda_{em.}$ = 584 (**1**)/582(**2**)/593(**3**) nm and emission spectra with $\lambda_{exc.}$ = 390 nm (**1** and **2**) and 393 nm (**3**).

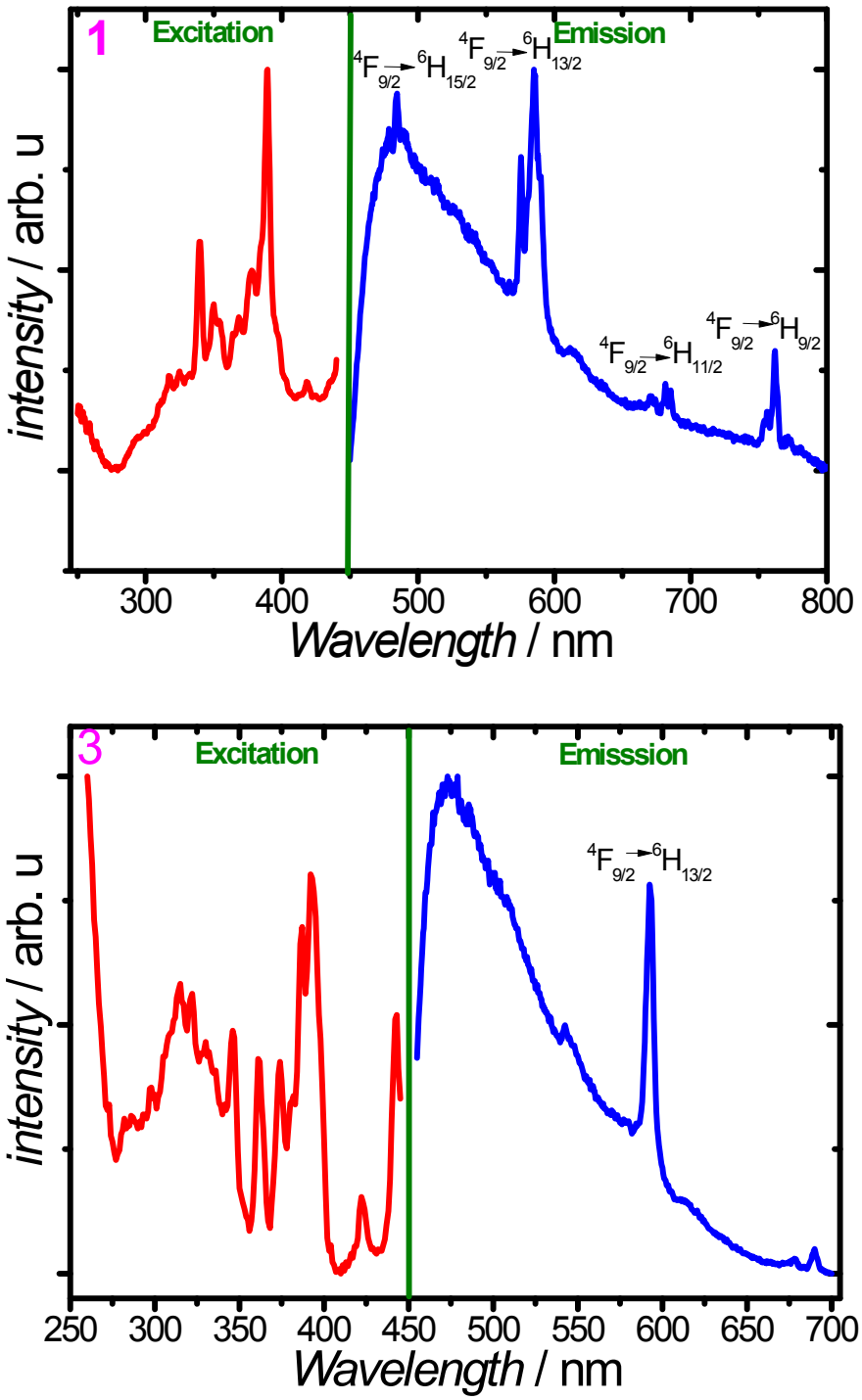

Figure S15: Low temperature (77 K) normalized excitation spectra monitored at $\lambda_{em.}$ = 584 (**1**) and 593 (**3**) nm and emission spectra at $\lambda_{exc.}$ = 390 (**1**) and 393 (**3**) nm.

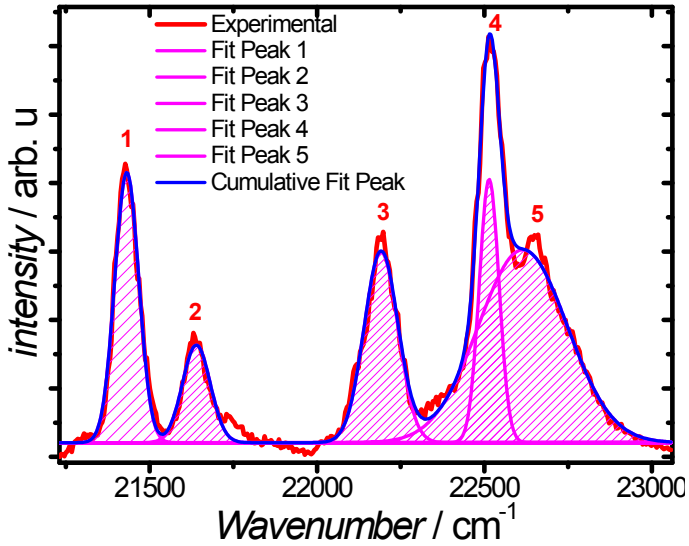

Figure S16: High-resolution excitation spectra monitored at $\lambda_{em.}$ = 582 nm for **2** showing a Gaussian deconvolution in five different peaks.

Table S1: Crystal data, data collection and structure refinement details for **1-3**.

	1	**2**	**3**
Formula	$C_{24}H_{32}DyF_{18}O_6$, $C_{24}H_{20}B$, ½C_4H_8O	$C_{44}H_{40}DyF_{18}O_7$, $C_{24}H_{19}B$, 2½C_4H_8O	$C_{36}H_{48}DyF_{10}O_7$, $C_{24}H_{20}B$, 2C_4H_8O
M	1276.25	1683.72	1408.66
T, K	100	120	110
Crystal system	Orthorhombic	Monoclinic	Monoclinic
Space group	*Pnma*	$P2_1/c$	*C2/c*
Z (Z')	8 (1)	4 (1)	8 (1)
a, Å	19.0304(2)	12.9539(13)	18.8988(3)
b, Å	24.9486(3)	24.207(2)	17.6320(3)
c, Å	22.2887(2)	23.410(2)	38.9502(6)
α, °	90	90	90
β, °	90	92.820(2)	95.056(2)
γ, °	90	90	120
V, Å^3	10582.27(19)	7331.8(12)	129128.6(4)
d_{calcd}, g·cm^{-3}	1.602	1.525	1.447
μ, mm^{-1}	1.524	1.123	1.241
F_{000}	5128	3424	5800
$2\theta_{max}$, °	52.04	52.00	52.04
Number of measured refl.	128769	47737	27770
Number of independent refl. (R_{int})	10688 (0.0685)	14392 (0.1365)	12690 (0.0283)
Observed refl. [$I > 2\sigma(I)$]	7455	7855	10557
Parameters	1104	1049	1019
R_1 [$I > 2\sigma(I)$]	0.0438	0.0611	0.0466
wR_2 (all data)	0.1036	0.1574	0.1140
$S(F^2)$	1.005	1.015	1.062
Residual density (d_{min}/d_{max}), e·Å^{-3}	1.21 / -1.54	1.42 / -1.38	1.21 / -0.79

Table S2: SHAPE analysis for **2** and **3**.

	HP	**HPY**	**PBPY**	**COC**	**CTPR**	**JPBPY**	**JETPY**
2	33.974	22.163	2.780	2.538	1.620	4.808	20.523
3	34.109	24.365	0.461	8.226	6.344	1.699	23.769

HP: Heptagon
HPY: Hexagonal pyramid
PBPY: Pentagonal bipyramid
COC: Capped octahedron
CTPR: Capped trigonal prism
JPBPY: Johnson pentagonal bipyramid J13
JETPY: Johnson elongated triangular pyramid J7

Table S3: Fitting of the Cole-Cole plots with a generalized Debye model under a zero dc field for **1**.

T (K)	χ_S (cm^3. mol^{-1})	χ_T (cm^3. mol^{-1})	α
2	1.53402	5.49115	0.35185
6	0.59725	1.87565	0.31181
10	0.39032	1.11268	0.24857
14	0.28948	0.79268	0.22817
18	0.22859	0.62486	0.24336
20	0.20476	0.5657	0.25617
22	0.18468	0.51834	0.26587
24	0.16735	0.47826	0.27212
26	0.15306	0.44595	0.28661
28	0.13756	0.41755	0.29545
30	0.12607	0.39168	0.29996
32	0.11694	0.37122	0.30499
33.6	0.11865	0.35383	0.26819
35.2	0.11198	0.33788	0.25049
36.8	0.10975	0.32294	0.19697
38.4	0.10728	0.31029	0.15633
40	0.10061	0.2984	0.14583
41.5	0.09867	0.28843	0.13556
43	0.09041	0.28004	0.1431
44.5	0.08957	0.27088	0.1426
46	0.08769	0.26243	0.15715
47.5	0.09537	0.25538	0.13819
49	0.10024	0.24726	0.11695
50.5	0.08289	0.24056	0.14701
52	0.09144	0.23392	0.12071

Table S4: Fitting of the Cole-Cole plots with a generalized Debye model for temperature ranging under a zero dc field for **2**.

T (K)	χ_S (cm^3. mol^{-1})	χ_T (cm^3. mol^{-1})	α
2	0.227	7.25	0.358
5	0.163	2.76	0.299
10	0.104	1.33	0.267
15	0.0749	0.878	0.255
20	0.0563	0.663	0.26
22	0.0534	0.604	0.262
24	0.0502	0.553	0.254
26	0.0451	0.511	0.253
28	0.044	0.475	0.246
30	0.0421	0.444	0.245
32	0.0382	0.418	0.246
34	0.0353	0.393	0.244
36	0.0354	0.371	0.231
37	0.0354	0.36	0.226
38.5	0.0286	0.346	0.228
40	0.0324	0.331	0.197
41.5	0.0573	0.292	0.202
43	0.0201	0.308	0.197
44.5	0.0273	0.296	0.15

Table S5: Fitting of the Cole-Cole plots with a generalized Debye model for temperature ranging under a zero dc field for **3**.

T (K)	χ_S (cm^3. mol^{-1})	χ_T (cm^3. mol^{-1})	α
17.4989	0.24443	0.6515	0.35351
24.9995	0.19198	0.43075	0.22303
32.4996	0.16067	0.33196	0.1574
39.9998	0.1365	0.27365	0.14079
47.4994	0.11976	0.23681	0.1405
54.9984	0.10273	0.21279	0.23172
62.4979	0.0786	0.20291	0.37365
69.9979	0.06512	0.21497	0.44346
71.9973	0.07189	0.20754	0.36748
73.9969	0.07738	0.20033	0.26243
77.996	0.07481	0.19154	0.19093
79.9959	0.07501	0.18604	0.14347
81.9971	0.07098	0.18235	0.16096
83.9952	0.07129	0.17921	0.12728
85.9984	0.07317	0.17383	0.09705
87.9954	0.04023	0.1723	0.19401
89.9978	0.04112	0.16814	0.20857

Table S6: Fit parameters of the field dependence of the relaxation time at 30 K for **1** and **2**.

Compound	***D*** ($s^{-1}K^{-1}Oe^{-4}$)	***B_1*** (s^{-1})	***B_2*** (Oe^{-2})	***K***
1 (30 K)	1.01×10^{-15}	195.5	9.1×10^{-6}	540.1
2 (30 K)	1.14×10^{-16}	71.0	4.1×10^{-5}	107.8
3 (40 K)	2.12×10^{-16}	31.9	1.4×10^{-5}	85.6

Table S7. Fitting of the Cole-Cole plots with a generalized Debye model under a 1000 Oe dc field for **1.**

T (K)	χ_S ($cm^3. mol^{-1}$)	χ_T ($cm^3. mol^{-1}$)	α
10	0.38656	0.97054	0.10623
14	0.28882	0.71587	0.1315
18	0.22666	0.59052	0.19482
20	0.20499	0.54514	0.22013
22.5	0.18247	0.49619	0.24045
25	0.15922	0.45668	0.27452
27.5	0.14781	0.41935	0.27205
30	0.12893	0.38859	0.23994
32	0.11932	0.36675	0.27499
33.5	0.11621	0.35148	0.25828
35	0.11621	0.35148	0.25828
36.5	0.11141	0.32315	0.18386
38	0.11047	0.31157	0.14721
39.5	0.10587	0.30000	0.12147
41	0.09613	0.29019	0.14259
42.5	0.09657	0.2802	0.13415
44	0.09629	0.27214	0.13183
45.5	0.09326	0.2639	0.13643
47	0.09947	0.25646	0.12833
48.5	0.09141	0.24782	0.1413

Table S8. Fitting of the Cole-Cole plots with a generalized Debye model under a 1000 Oe dc field for **2.**

T (K)	χ_S (cm^3. mol^{-1})	χ_T (cm^3. mol^{-1})	α
20	0.05629	0.70261	0.26076
22	0.05193	0.64603	0.27076
24	0.04775	0.59089	0.26426
26	0.04562	0.54063	0.25095
28	0.03827	0.50568	0.26368
30	0.03975	0.46898	0.24895
32	0.03442	0.43914	0.2463
34	0.039	0.41144	0.22582
36	0.033	0.38719	0.21998
37	0.03281	0.37703	0.22591
38.5	0.03134	0.36089	0.20852
40	0.02821	0.34619	0.20406
41.5	0.03342	0.33383	0.17699
34	0.01918	0.32159	0.19017
44.5	0.03516	0.30972	0.14721

Table S9. Fitting of the Cole-Cole plots with a generalized Debye model under a 1000 Oe dc field for **2.**

T (K)	χ_S (cm^3. mol^{-1})	χ_T (cm^3. mol^{-1})	α
27.14288	0.17384	0.38425	0.15036
41.42824	0.12025	0.25674	0.14036
48.57047	0.10276	0.22358	0.17453
55.71231	0.09339	0.19924	0.19334
62.85474	0.07774	0.18819	0.29281
69.99895	0.05789	0.20178	0.42599
71.99842	0.05823	0.19564	0.34738
73.99617	0.06713	0.18966	0.26902
75.99703	0.06526	0.18317	0.20831
77.99517	0.06226	0.17846	0.18221
79.99618	0.05527	0.1752	0.19563

81.99704	0.05867	0.17035	0.14327
83.99694	0.05059	0.16723	0.16064
85.99476	0.04654	0.16383	0.13844
87.99646	0.01646	0.15848	0.26486
89.99459	1.41041E-14	0.15866	0.25522
91.99635	0.0157	0.15219	0.13698

Table S10. Fit parameters of the temperature dependence of the relaxation time for **1-3**.

Compound	$\Delta (cm^{-1})$	τ_0 (s)	m	C ($s^{-1}.K^{-m}$)
1 (1000 Oe)	184 ± 10	$(8 \pm 2) \times 10^{-7}$	2*	0.32 ± 0.07
2 (1000 Oe)	470 ± 13	$(4 \pm 2) \times 10^{-11}$	2.1*	0.06 ± 0.02
3 (1000 Oe)	1534 ± 121	$(3 \pm 5) \times 10^{-15}$	2.1*	0.04 ± 0.01

** fixed parameter*

Table S11. Estimation of the relaxation time and temperature switch.

	τ_{switch} (s)	T_{switch} (K)
1	6.40×10^{-4}	36.6
2	1.91×10^{-3}	37.2
3	1.12×10^{-3}	80.3
$[Dy(OCPh_3)_2(THF)_4][BPh_4]$[3]	1.04×10^{-3}	85.1

Table S12. Crystal-field splitting of the $^4F_{9/2}$ obtained by luminescence and their relative Boltzmann population at 77 K.

$^4F_{9/2}$ doublets	*Energy* (cm^{-1})	*Relative population at 77 K*
1	0	0.97586988
2	198	0.02412942
3	758	6.8855E-07
4	1078	-
5	1175	-

References

1 K. Randall McClain, C. A. Gould, K. Chakarawet, S. J. Teat, T. J. Groshens, J. R. Long and B. G. Harvey, *Chem. Sci.*, 2018, **9**, 8492-8503.

2 D. Reta and N. F. Chilton, *Phys. Chem. Chem. Phys.*, 2019, **21**, 23567-23575.

3 J. Long, A. O. Tolpygin, E. Mamontova, K. A. Lyssenko, D. Liu, M. D. Albaqami, L. F. Chibotaru, Y. Guari, J. Larionova and A. A. Trifonov, *Inorg. Chem. Front.*, 2021, **8**, 1166-1174.